Dependence of non-reciprocity in spin wave excitation on antenna configuration

This manuscript was accepted by J. Appl. Phys. Click here to see the version of record.

Koji Shibata[1], Kenji Kasahara[1], Kazuyuki Nakayama[1], Volodymyr V. Kruglyak[2], Mustafa M. Aziz[3], and Takashi Manago[1, 2*]

[1] *Department of Applied Physics, Fukuoka University, Fukuoka 814-0180, Japan*

[2] *Department of Physics and Astronomy, University of Exeter, Exeter EX4 4QL, UK*

[3] *College of Engineering, Mathematics and Physical Sciences, University of Exeter, Exeter EX4 4QF, UK*

*E-mail: manago@fukuoka-u.ac.jp

The dependence of nonreciprocity of excitation of magnetostatic surface waves (MSSW) on antenna width was investigated experimentally and theoretically. The nonreciprocity was successfully modified by changing the excitation antenna width. The nonreciprocity ratio, which was defined as the spin wave intensity under negative bias field divided by that under positive bias field, was found to decrease with increasing antenna width. Micromagnetic simulations revealed that this decrease in the nonreciprocity ratio originates from the rapid decrease in the in-plane excitation field compared to the perpendicular excitation field with reducing the antenna width.

1. Introduction

The emerging field of magnonics has gained significant interest, ranging from fundamental studies of spin wave properties to their application for the information transport and processing in complex device architectures.[1-7] An important perceived advantage of using spin waves is the low power consumption for information transport, due to the lack of necessity to transport charge with inevitable Joule heating. One of the spin wave modes, magneto-static surface wave (MSSW), has been investigated intensively owing to its large signal and so increased propagation length in metal systems. Here, we focus on the nonreciprocity characteristics of the MSSW excitation, i.e. the difference in the intensity of excited spin waves depending on their propagation direction. The nonreciprocity of MSSWs and its potential applications have been addressed in a number of recent studies.[8-14] For instance, based on yttrium-iron-garnet (YIG) films, various MSSW devices have been developed, such as band pass filters, circulators, and isolators, which utilize the strong nonreciprocity of MSSWs.[15-17] In addition, a logic device exploiting the interference of MSSWs in permalloy films was reported.[18] In order to obtain a firmer control of the on/off ratio in this logic device, it is essential to set the same intensity of spin waves propagating in the opposite direction. At the same time, theoretical attempts to achieve unidirectional spin wave emission have suggested the Dzyaloshinskii-Moriya interaction[19-21] as an alternative means to control the relative strength of spin-wave excitation for opposite propagation directions. Thus, control of the spin-wave excitation nonreciprocity is important to develop logic architectures and various other high-performance devices based on spin waves.

There are two types of nonreciprocity for MSSW, one affecting the distribution of the dynamic magnetization through the film thickness and the other related to the intensity difference depending on the propagation direction. The maximum of the dynamic magnetization shifts from one side of the film to the other when the direction of propagation is reversed, exhibiting the exponential decay $\exp(-ky)$ where k is a wave vector and y is a distance from the surface of the film.[22, 23] But in a thin metal film of thickness d such as 50 nm and a low wave vector of about 0.3 μm^{-1} (observed in our experiments), kd is of the order of 10^{-2}, which is enough small to neglect the magnetization distribution difference through the thickness of the film. On the other hand, the intensity difference is caused by the difference in phase excited by the microwave transducer. The nonreciprocity of MSSW excitation by microwave antennae occurs due to superposition of waves excited by the antenna's magnetic fields normal to the film plane and to the in-plane component of the magnetization. The

This manuscript was accepted by J. Appl. Phys. Click here to see the version of record.

amplitudes of the dynamic magnetization $m_{\pm}$ excited by the antenna's field for the positive (+) and negative (−) directions of the bias magnetic field may be expressed as[8,14]

$$m_{\pm} \propto \frac{2\pi f}{M_S \gamma} \pm \frac{1}{M_S{}^2}\left[\left(\frac{2\pi f}{\gamma}\right)^2 - (\mu_0 H)^2\right], \qquad (1)$$

where f is the spin-wave frequency, M_S is the saturation magnetization, γ is the gyromagnetic ratio, and H is the bias magnetic field. This equation was derived assuming the dynamic magnetization is averaged through the film thickness. The first and second terms in Eq. (1) are due to the in-plane component (x-component), h_x, and the out-of-plane component (z-component), h_z of the antenna's magnetic field, respectively. The coordinate system is defined in Fig. 1(a). Hence, by defining the corresponding dynamic magnetization terms as m_{hx} and m_{hz}, $m_{\pm}$ can be written as $m_{\pm} = m_{hx} \pm m_{hz}$. Furthermore, we define the nonreciprocity ratio NR as a ratio of m_{-} to m_{+}, i.e,

$$NR = \frac{m_{-}}{m_{+}} = \frac{m_{hx} - m_{hz}}{m_{hx} + m_{hz}} \qquad (2)$$

In this formulation, the NR is 100% when there is no difference between m_{-} to m_{+}, while greater differences between m_{-} to m_{+} yield smaller values of NR. According to Eq. (1), NR is mainly determined and so may be controlled by the magnetic parameters of the sample and / or by the spin-wave frequency. However, the dynamic magnetization terms m_{hx} and m_{hz} in Eq. 1 were derived using the same intensity of the excitation field for both components, and so, they do not take into account the antenna configuration or excitation area in Schneider's formulation.[8] Therefore, modulation of each component of the dynamic magnetization by the antenna configuration could control the nonreciprocity of the MSSW excitation. Previously, we reported the dependence of the nonreciprocity on the distance between the magnetic layer and excitation antenna, where we showed that the nonreciprocity can be changed by changing the thickness of the separating insulating layer.[14] This result indicates the importance of the excitation antenna configuration for the MSSW excitation nonreciprocity. Changing the excitation antenna width could also change the contributions of m_{hx} and m_{hz}, and therefore the nonreciprocity of the MSSW emission. In this paper, we report the dependence of the nonreciprocity on the excitation antenna width, both experimentally and theoretically.

2. Experimental methods

2.1 Spin wave measurements

Permalloy (Py) strips with dimensions 600 × 100 μm were formed on a SiO_2/Si substrate using

e-beam lithography and e-beam evaporation techniques. The thickness of the strips was 50 nm. They were covered with an 80 nm thick SiO_2 insulating layer by sputtering, on top of which Cr (5 nm) / Au (200 nm) coplanar waveguides (CPWs) of signal-ground (SG) type were formed. The sample configuration is schematically shown in Fig. 1(a) and (b). The ratio of the widths of the signal line (S) and ground line (G), and the SG-gap was 1:3:1. A series of samples was prepared in which the width of signal line (W_a) was 1, 2, 4, 8, and 16 μm. The edge-to-edge distance between the excitation and detection antennae was 10 μm. The transmitted spin-wave signals S_{21} were measured by a vector network analyzer (HP-8510C) and a microprobe station (Cascade Microtech Summit 9000) at room temperature. The input power was 0 dBm. An electromagnet was used to apply an in-plane external bias magnetic field perpendicular to the spin-wave propagation direction, as shown in Fig. 1(a). Hence, the spin waves excited and studied in this geometry are MSSWs. Spin-wave signals were obtained by subtracting a background signal measured in a high magnetic field of 300 mT. Hereafter, we use the subtracted signal ΔS_{21} to indicate the spin wave signal. To estimate the nonreciprocity of the MSSW excitation, the bias magnetic field direction was reversed instead of reversing the propagation direction. In a separate measurement, we confirmed that both methods gave the same nonreciprocity results. Additionally, we set the experimental arrangement in which the sign of the bias magnetic field matched the sign of the dynamic magnetization m_+ and m_- in Eq. (1). When the antenna width W_a is changed, this also changes the wave vector of the propagating spin wave that is excited by the antenna. Then, if the bias magnetic field is fixed, the resonance frequency (f_r) of the device also changes. Hence, to compare the excitation nonreciprocity for samples with different W_a, we have to set the same f_r so as to maintain a consistent wave vector, because the nonreciprocity depends on frequency.[13] We achieved this by adjusting the bias magnetic field. For each sample, the nonreciprocity was then measured at frequencies f_r = 5, 6 and 7 GHz.

2.2 Micromagnetic simulations

Micromagnetic simulations of the spin wave propagation were performed using the Object Oriented Micromagnetic Framework (OOMMF) software package, which is based on the Landau-Lifshitz equation

$$\frac{d\boldsymbol{M}}{dt} = -\gamma \boldsymbol{M} \times \boldsymbol{H}_{\text{eff}} - \frac{\gamma\alpha}{M_S} \boldsymbol{M} \times (\boldsymbol{M} \times \boldsymbol{H}_{\text{eff}}) \quad (3)$$

where $\boldsymbol{M}$ is the magnetization, $\boldsymbol{H}_{\text{eff}}$ is the effective field, γ is the Landau-Lifshitz gyromagnetic

ratio, and α is the damping constant.[24] Py strips with dimensions of 102.4 μm × 6 μm × 50 nm were discretized into 50 nm cubic cells. Periodic boundary conditions were applied along the y-axis, so as to eliminate the demagnetizing field due to a finite strip width. The dispersion of the MSSWs in the relevant wavelength range is dominated by the magneto-dipole interaction. So, our chosen cell size is sufficient for an adequate description of the MSSWs. In a separate simulation, we verified that the use of smaller cells does not modify the results significantly. The simulation parameters were M_S = 830 kA/m, γ = 2.337 × 10^5 m/(A·s), α = 0.01, exchange stiffness constant A = 1.3 × 10^{11} J/m and simulation time step of 10 ps. The bias magnetic field was determined using the relationship between the antenna configuration[25] and the dispersion relation of MSSWs, so that the peak frequency of the spectrum becomes equal to f_r. The distance between the signal and ground lines determines the dominant wavelength and the associated dominant wave vector k of the excited spin waves. It can be noticed that $m_\pm$ in Eq. (1) depends not only on the frequency but also on the bias magnetic field. However, the term $(2\pi f/\gamma)^2$ is much greater than $(\mu_0 H)^2$, and so, this latter field term is negligible, as we confirmed experimentally and theoretically in our previous report.[13] Therefore, it is important to compare NR values at the same frequency. The excitation field of the SG type antenna was separately calculated using MATLAB. The in-plane and perpendicular components of the magnetic field created by an antenna strip with a rectangular cross section were given by Eq. (5) and (6) in reference [26]. The SG type CPW consists of two individual wires. We assume that the current in the two wires is the same in value but opposite in sign. However, the current densities in the signal and ground wires are different because they have different widths. The magnetic field of the CPW was calculated by adding the fields created by these two individual wires. As an example, Fig. 1(c) shows the profiles of the x- and z-components of the magnetic field for the antenna with a 2 μm wide signal and 6 μm wide ground lines. Hereafter, we call h_x as the x-component of the antenna field and h_z as the z-component of the antenna field. Using the calculated field profiles, a Gaussian pulse excitation with a pulse width of 50 ps was applied in OOMMF. The pulsed excitation is suitable to excite spin waves over a wide range of frequencies all at once, and the spin-wave spectra can be obtained by Fast Fourier Transformation (FFT).[27] The extracted data only includes the out-of-plane component (z-component) of the dynamic magnetization, which is sufficient for our analysis. To evaluate the nonreciprocity, the external bias field was reversed, and the obtained results were compared.

3. Results and discussion

Experimental spin-wave spectra with f_r = 6 GHz are shown in Fig. 2. Excitation antenna with narrower widths generate broader spectra. So, we kept the resonance frequency f_r at 6 GHz by using an individually adjusted magnitude of the bias magnetic field for different samples. The intensity of excited spin waves decreases as W_a increases. This is because the current density in the antenna and therefore the antenna's magnetic field both decrease as W_a increases. Fig. 2 shows that the intensity of spin waves excited under positive field is greater than that under the negative field. Thus, the nonreciprocity in the excited spin-wave intensity is clearly observed for all samples. In the definition of *NR* in Eq. (2), a smaller difference of the intensities leads to a greater value of *NR*. If there is no difference of the intensity, the *NR* becomes unity (or 100%). Fig. 3 shows the W_a dependence of the *NR* at frequencies 5, 6 and 7 GHz. For the same antenna width, the *NR* decreases as the frequency increases, which is consistent with the previous result.[13] As W_a is varied, the *NR* initially increases with W_a, but then decreases for antennae widths of W_a = 4 μm and greater. Thus, *NR* can be changed by the antenna configurations. However, if the ratio of the excitation areas of h_x and h_z influences the nonreciprocity, greater W_a values should lead to greater values of m_{hx}, and therefore to greater *NR* values (i.e. smaller asymmetry). The presented experimental results do not support this intuitive speculation.

NR was also investigated using micromagnetic simulation to understand the experimental measurements. Simulated time dependent waveforms were converted into spin-wave spectra by application of the FFT at each cell. A typical intensity map of the spin wave spectra along the *x*-axis (propagation direction) is shown in Fig. 4(a). These spectra peak at frequencies around f_r = 6 GHz for 2 μm antenna. The left dashed line at x = 1 μm represents the excitation antenna edge. The other dashed line at x = 12 μm corresponds to the center of the detection antenna (recall that the edge-to-edge distance between antennae is 10 μm and the antenna width is 2 μm). The inset shows the spin wave spectrum at x = 12 μm, which has a shape similar to the experimental result in Fig. 2. Fig. 4(b) presents the *NR* map, which is obtained by calculating the ratio of the m_- map/m_+ map. *NR* in the region below the spin wave spectrum shows almost 100% because there are no propagating spin waves in this region. So, the calculated values of m_- and m_+ are almost the same, and so, m_-/m_+ becomes 100% (recall that *NR* of 100% means no difference in the intensities for m_- and m_+). *NR* in the higher frequency region decreases with frequency, and the *NR* variation along the *x*-axis at the peak frequency of the spectra (inset) shows that the *NR* is almost constant. These results are also consistent with our previous reports.[13]

The W_a dependence of the calculated *NR* is summarized in Fig. 5. The *NR* values were obtained by averaging over the detection antenna width. Additionally, in the case of the peak frequency of the spectra being different between the results under positive and negative external fields (though it is a slight difference, if any), *NR* was calculated using each peak value. Qualitatively, Fig. 5 shows the same non-monotonic dependence of *NR* upon W_a as observed experimentally. However, the calculated absolute values are greater than those in the experiment, and the maximum of *NR* happens at $W_a = 2$ μm.

To understand the origin of these observations, we performed simulations in which spin waves were excited either only by h_x or only by h_z. Fig. 6 shows the waveforms of m_{hx} and m_{hz} excited by h_x and h_z, respectively, for a 2 μm wide antenna at $x = 12$ μm. When the external field is reversed ($-H$), the phase of m_{hx} is shifted by π, whereas m_{hz} remains identical to that before the field reversal. As a result, the dynamic magnetizations of m_{hx} and m_{hz} under the positive field are in-phase and strengthen each other, but those under negative field are out-of-phase and weaken each other. The superposition of these waves makes up the spin waves observed in the experiment, and this is the origin of the MSSW excitation nonreciprocity, which was also reported using micromagnetic simulations elsewhere.[11] The *NR* value estimated by these superimposed wave spectra is the same as the simulation results shown in Fig. 5.

Fig. 7(a) shows the dependence of the maximum values of the excitation fields, h_x and h_z (indicated in Fig. 1(c)) on the excitation antenna width W_a. Fig. 7(b) shows theW_a dependence of the FFT of m_{hx} and m_{hz}. As shown in Fig. 7(a), the decrease of h_x maximum with increasing W_a is more rapid than the decrease of h_z maximum. Correspondingly, in Fig. 7 (b), the FFT of m_{hx} also decreases more rapidly than the FFT of m_{hz}, which leads to the *NR* decrease (i.e. greater nonreciprocity). Thus, qualitatively, the reduction of the *NR* originates from the rapid decrease in the in-plane excitation field compared to the perpendicular excitation field with increasing W_a. Fig. 7(c) shows the ratio of the maximum dynamic magnetization m_{hx} and m_{hz} after excitation and its excitation field h_x and h_y, respectively. These values represent the excitation efficiency by each field component. The insets in Fig. 7(c) are the antenna fields for spin wave excitations for W_a values of 1, 2 and 4 μm. For h_x excitation, there is a general reduction in magnitude of the magnetic field in the corner and central regions of the conductors with increasing antenna width that is not matched by reduction in the in-plane magnetization leading to the increase of the excitation efficiency. On the other hand, for h_z excitation, the reduction of the magnetic field in the corner and surrounding regions of the conductor lead to further reductions in the unfavourable out-of-plane magnetization leading to the decrease of the

excitation efficiency. Therefore, for small antennae widths, m_{hx} does not decrease very much regardless of the decrease of h_x, and m_{hz} declines more than the decrease of h_z. This causes the increase in the *NR* and the observed non-monotonic dependence of the nonreciprocity on the antenna width. Thus, the speculation that nonreciprocity could depend on the ratio of excitation area of h_x and h_z is not valid as previously assumed,[14] because spin waves have a certain group velocity and spin waves excited at a sufficiently far distance from each other do not interfere.

4. Conclusions

In summary, the antenna width dependence of *NR* was investigated experimentally and theoretically. *NR* increases initially for small antenna widths W_a but tends to decrease with increasing antenna width W_a beyond a certain value. This tendency was obtained not only in the experiment but also in micromagnetic simulations in this work. The reduction of *NR* appears to originate from the rapid decrease in the in-plane excitation field compared to the perpendicular excitation field with increasing W_a. The origin of the non-monotonic dependence of *NR* on the antenna width is due to the change of the excitation efficiency depending on the antenna width. The micromagnetic simulation results in this work qualitatively explain the experimental observations, however there is a slight difference between the experimental and calculated values. The numerical simulations in this paper do not include the effects of the electrical conductivity and dynamic permeability of the Py film. These could influence the spatial distribution of the excitation magnetic fields because this distribution should be modified by the vicinity of a ferromagnetic film and skin effects. Additionally, the effect of the induced current in the detection antenna by spin waves is not included in the micromagnetic calculations, and may affect the spin wave propagation, and so, the detection efficiency could depend on the antenna width. Calculations including all the factors listed above are necessary to understand these nonreciprocal behaviors in greater detail.

Acknowledgments

This work was partly supported by JSPS KAKENHI Grant Numbers 24560034 and 15K06000. This work was supported in part by funds (Nos. 167003 and 175005) from the Central Research Institute of Fukuoka University.

References

1) V. V. Kruglyak, S. O. Demokritov, and D. Grundler,J. Phys. D **43**, 264001 (2010).

2) B. Lenk, H. Ulrichs, F. Garbs, and M.Münzenberg, Phys. Rep. **507**, 107 (2011).

3) Y. Au, M. Dvornik,O. Dmytriiev, and V. V. Kruglyak, Appl. Phys. Lett. **100**, 172408 (2012).

4) A. V. Chumak, A. A. Serga, and B. Hillebrands, Nature Commun.**5**,4700 (2014).

5) A. V. Chumak, V. I. Vasyuchka, A. A. Serga, and B. Hillebrands,Nat. Phys. **11**, 453 (2015).

6) N. Kanazawa, T. Goto, K. Sekiguchi,A. B. Branovsky, C. A. Ross, H. Takagi,Y. Nakamura, and M. Inoue, Sci.Rep.**6**, 30268 (2016).

7) L. J. Cornelissen, J. Liu, and B. J. V. Wees (2018), Phys. Rev. Lett.**120**, 097702(2018).

8) T. Schneider, A. A. Serga, T. Neumann, B. Hillebrands,and M. P. Kostylev, Phys. Rev. B**77**, 214411 (2008).

9) V. E. Demidov, M. P. Kostylev, K. Rott, P. Krzysteozko, G. Reiss, and S. O. Demokritov, Appl. Phys. Lett.**95**, 112509 (2009).

10) K. Sekiguchi, K. Yamada, S. M. Seo, K. J. Lee, D. Chiba, K. Kobayashi, and T. Ono, Appl. Phys. Lett. **97**, 022508 (2010).

11) P. Depramo. J. H. Kwon, and H. Yang, Curr. Appl. Phys. **14**, S129 (2014).

12) M. Jamali, J. H. Kwon, S. M Seo, K. J. Lee, and H. Yang, Sci. Rep. **3**, 03160 (2013).

13) M. Nakayama, K. Yamanoi, S. Kasai, S. Mitani, and T. Manago, Jpn. J Appl. Phys. **54**, 083002 (2015).

14) K. Kasahara, M. Nakayama, Y. Xiaorui, K. Matsuyama, and T. Manago, Jpn. J Appl. Phys. **56**, 010309 (2017).

15) J. D. Adam, L. E. Davis, G. F. Dionne, E. F. Schloemann, and S. N. Stitzer,IEEE Trans. Microwave Theory Tech. **50**, 721 (2002).

16) J. Wu, X. Yang, S. Beguhn, J. Lou, and N. X. Sun, IEEE Trans. MicrowaveTheory Tech. **60**, 3959 (2012).

17) V. G. Harris, IEEE Trans. Magn. **48**, 1075 (2012).

18) N. Sato, K. Sekiguchi, and Y. Nozaki, Appl. Phys. Express **6**, 063001 (2013).

19) J. LAN, W. Yu, R. Wu, and J. Xiao, Phys. Rev. X **5**, 041049 (2015).

20) X. Xing and Y. Zhou, NPG Asia Mater. **8**, e246 (2016).

21) T. Brächer, O. Boulle, and G. Gaudin, Phys. Rev. B **95**, 064429 (2017).

22) R. W. Damon and J. R. Eshbach, J. Phys. Chem. Solids **19**, 308 (1961).

23) D. D. Stancil and A. Prabhakar, Spin Waves Theory and Application, Springer Science + Business Media (2009), pp. 162-166.

24) M. Donahue, D. Porter, OOMMF User's Guide, Version, 1.0, NISTIR 6376, National

Institute of Standards and Technology, Gaithersburg, MD (Sept 1999), website: http://math.nist.gov/oommf.

25) V. Vlaminckand M. Bailleul (2010), Phys. Rev. B**81**, 014425 (2010).

26) D. Chumakov, J.McCord, R. Schäfer, and L. Schultz, Phys. Rev. B **71**, 014410 (2005).

27) M. Dvornik, Y. Au, and V. V. Kruglyak, Top. Appl. Phys. **125**, 101 (2013).

Figure captions

Fig. 1.(Color online) (a) Schematic spin wave sample configuration and (b) its cross-section around the excitation antenna. (c) Antenna field for spin wave excitation calculated by MATLAB.

Fig. 2.(Color online) Spin wave spectra with resonant frequency of 6 GHz for various samples with different antenna widths W_a. In order to produce the same resonant frequency, the applied external field was adjusted.

Fig. 3.(Color online) Antenna width dependence of nonreciprocity at the peak frequencies of 5, 6 and 7 GHz from experiment.

Fig. 4.(Color online) (a) FFT Intensity map of the spin wave spectra for a sample with 2 □m width antenna. External field is 17 mT and peak frequency is about 6 GHz. The inset is the spin wave spectra at x = 12 μm. (b) Map of the nonreciprocity ratio NR. The inset is the NR along the propagation direction at about 6 GHz.

Fig. 5.(Color online) Antenna width dependence of nonreciprocity at the peak frequencies of 5, 6 and 7 GHz in the simulation.

Fig. 6.(Color online) The waveforms of m_{hx} and m_{hz} at x = 12 μm excited by h_x and h_z, respectively. The antenna width is 2 □m. (a) Under positive external field. (b) Under negative external field.

Fig. 7.(Color online) (a) W_a dependence of the maximum intensity of the excitation fields, h_x and h_z. (b) W_a dependence of the FFT intensity of the dynamic magnetizations, m_{hx} and m_{hz}. (c) W_a dependence of the ratio of the maximum dynamic magnetization m_{hx} and m_{hz} after excitation and its excitation field h_x and h_y. These correspond to the excitation efficiency by each field component. Insets are antenna fields of spin wave excitation for various antenna width.

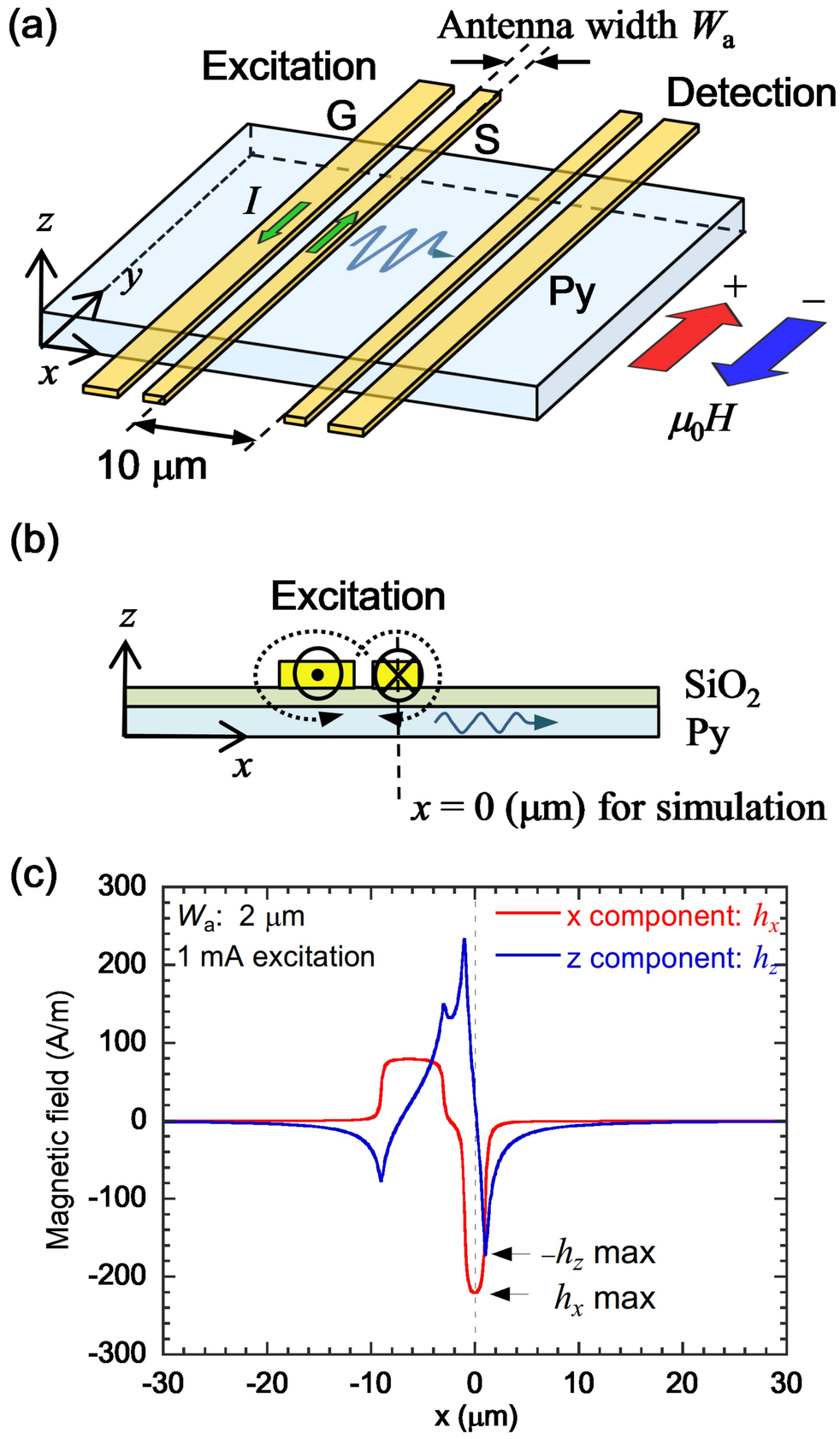

Fig. 1

This manuscript was accepted by J. Appl. Phys. Click here to see the version of record.

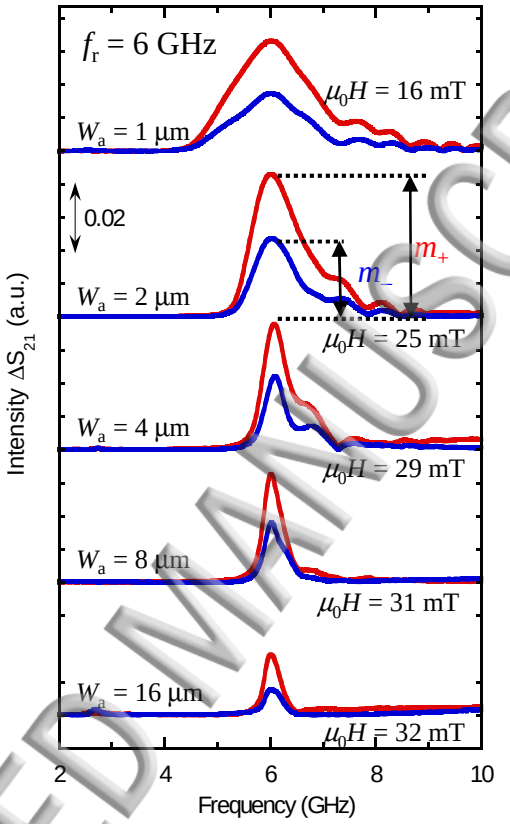

Fig. 2

This manuscript was accepted by J. Appl. Phys. Click here to see the version of record.

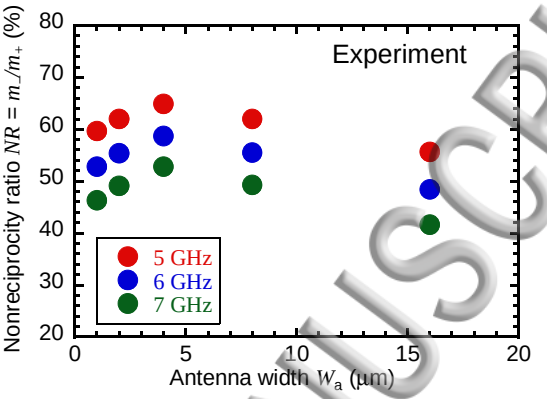

Fig. 3

This manuscript was accepted by J. Appl. Phys. Click here to see the version of record.

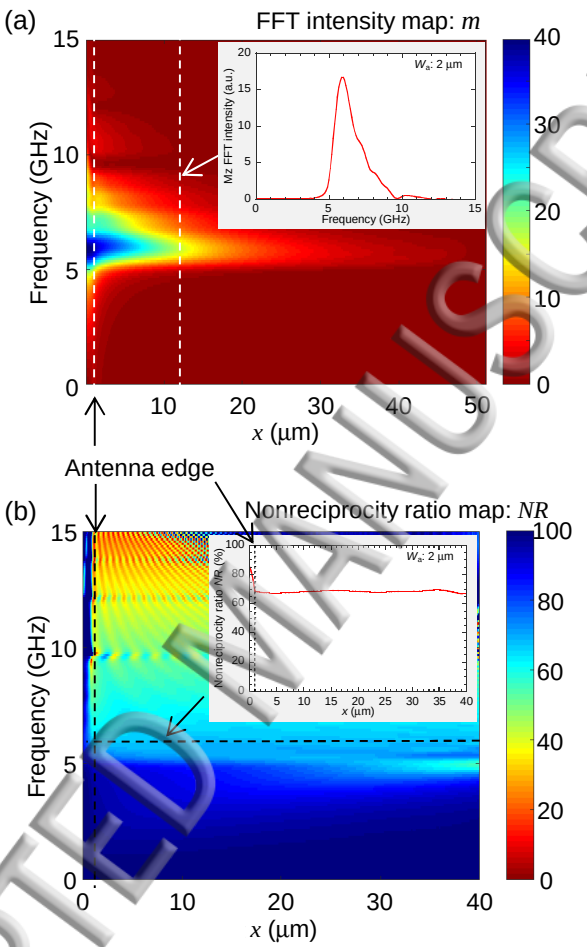

Fig. 4

This manuscript was accepted by J. Appl. Phys. Click here to see the version of record.

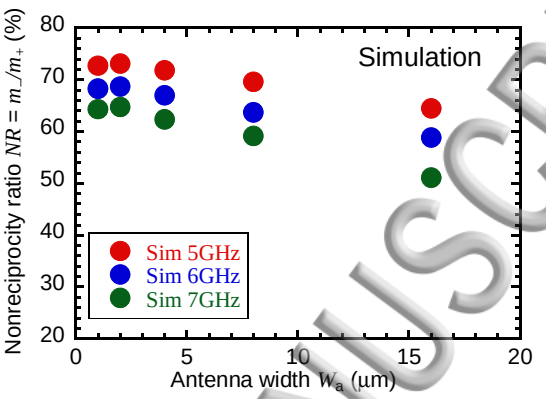

Fig. 5

This manuscript was accepted by J. Appl. Phys. Click here to see the version of record.

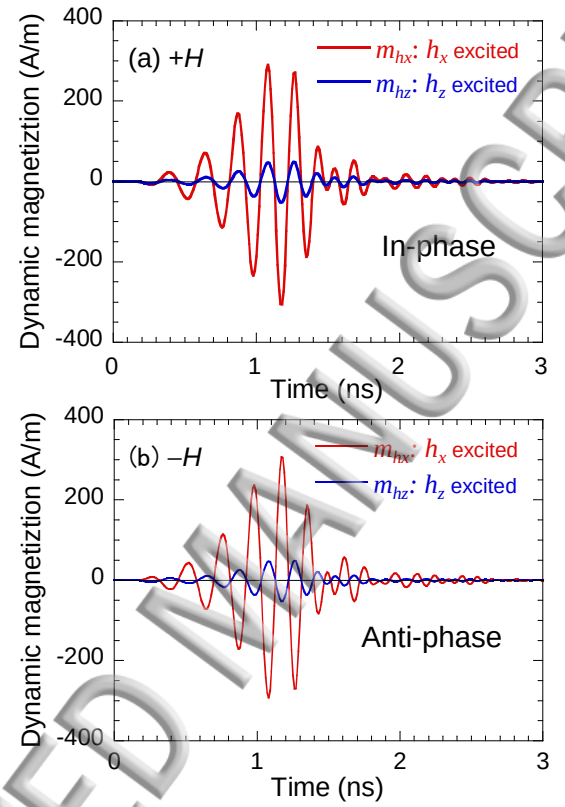

Fig. 6

This manuscript was accepted by J. Appl. Phys. Click here to see the version of record.

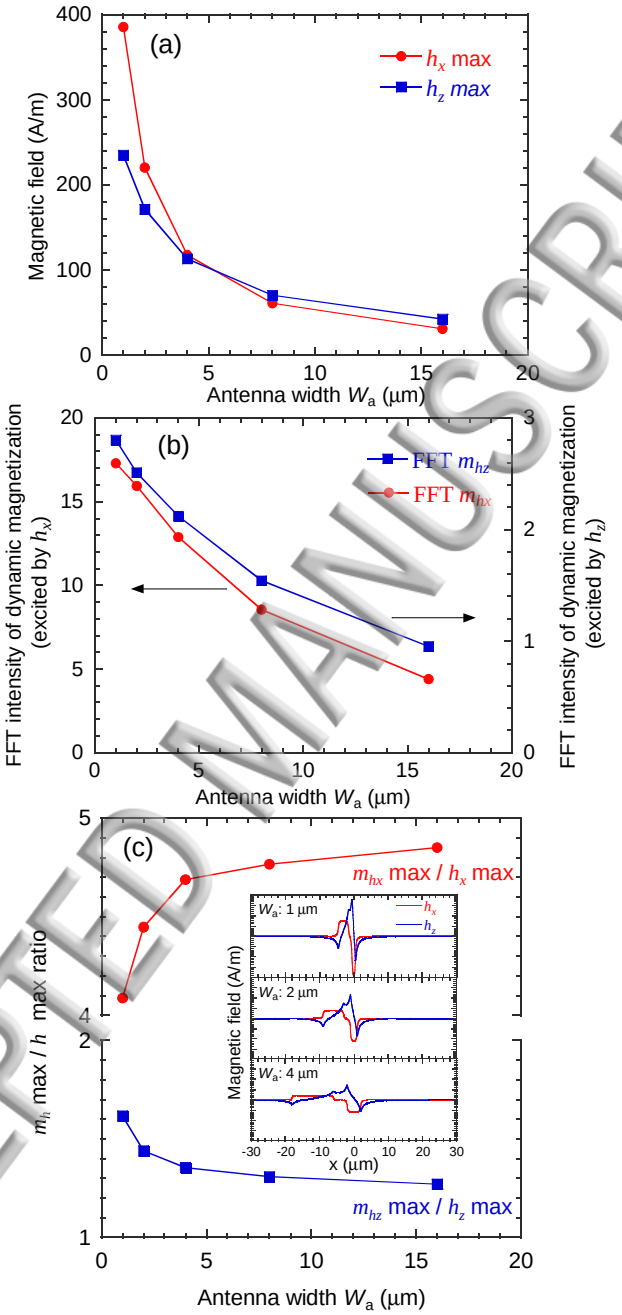

Fig. 7